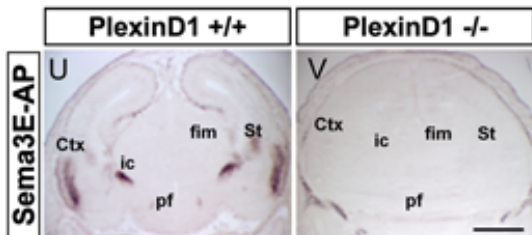
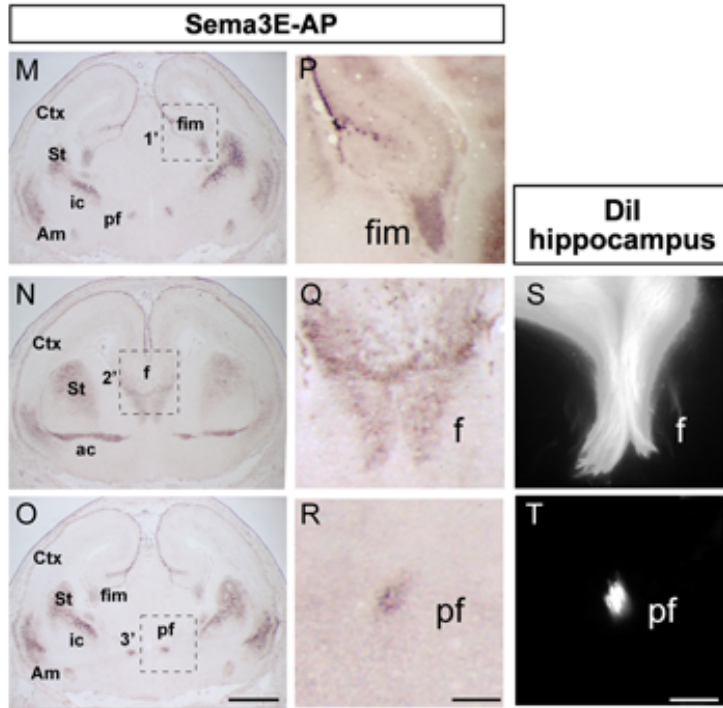
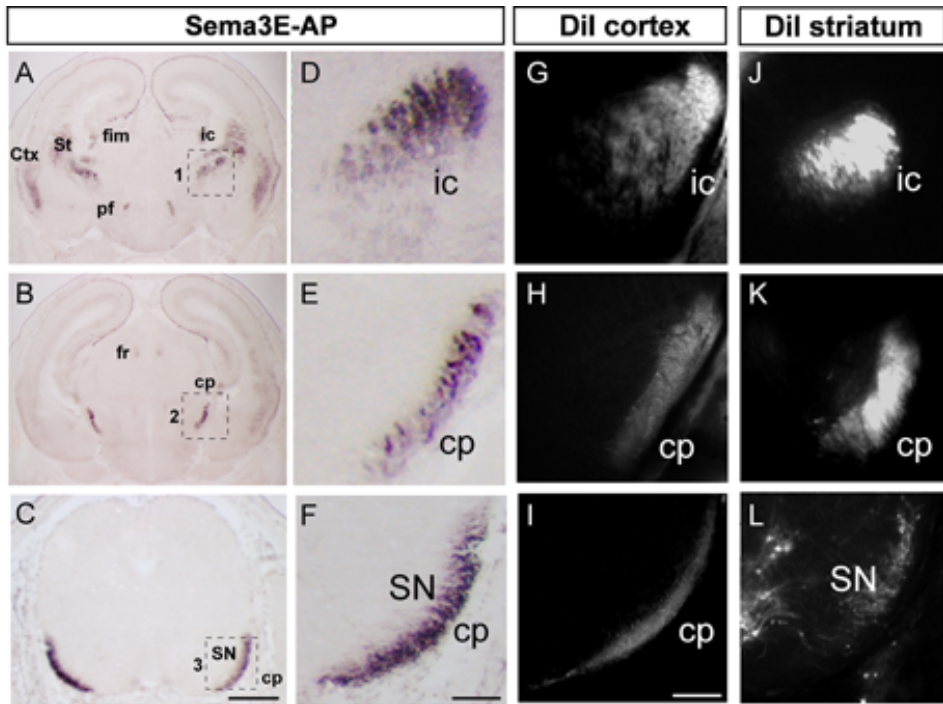


Neuron, Volume 56

Supplemental Data

**Gating of Sema3E/PlexinD1 Signaling by Neuropilin-1
Switches Axonal Repulsion to Attraction during Brain Development**

Sophie Chauvet, Samia Cohen, Yutaka Yoshida, Lylia Fekrane, Jean Livet, Odile Gayet, Louis Segu, Marie-Christine Buhot, Thomas M. Jessell, Christopher E. Henderson and Fanny Mann



Suppl. Fig. 1: Binding sites for Sema3E along the corticofugal, striatonigral and subiculo-mammillary tracts correlate with anterograde DiI labeling of each pathway

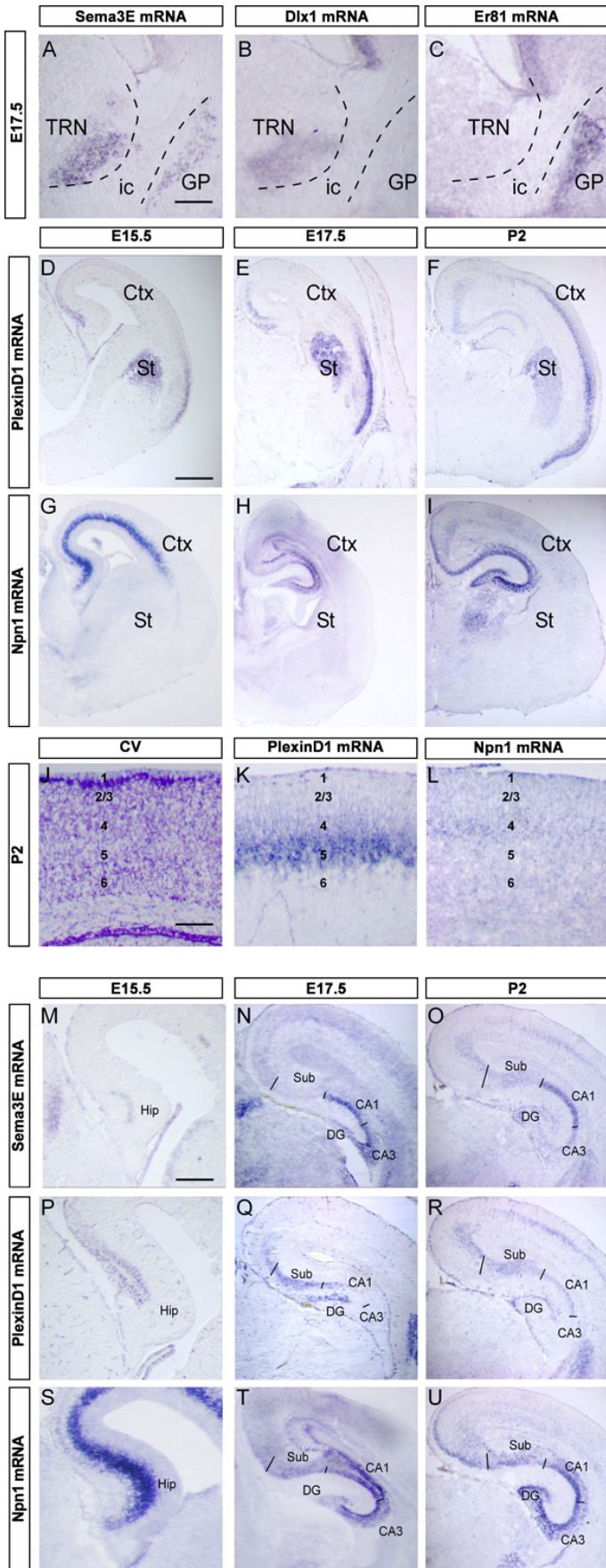
(A-F) Coronal sections of wild-type brain at E17.5 showing the localization of Sema3E binding sites along the corticofugal and striatonigral projections. (A-C) Binding of Sema3E-AP is apparent in the internal capsule (ic in C) and cerebral peduncles (cp in B, C). (D-F) Higher magnifications of the areas boxed in A-C. (G-I) High-magnification views of DiI labeled axons arising for ventrolateral regions of the cortex at different levels of the corticofugal projections: internal capsule (G) and cerebral peduncles (H, I). High-magnification views of DiI labeled striatonigral axons in the internal capsule (J), cerebral peduncle (K) and substantia nigra (SN in L). The observed patterns correlate tightly with the sites of Sema3E-AP binding.

(L-S) Coronal sections of wild-type brain at E17.5 showing localization of Sema3E binding partners along the subiculo-mammillary tract. (L-N) Binding of Sema3E-AP is apparent in the fimbria (fim in L), fornix (F in M) and postcommissural fornix (PF in N). (O-Q) Higher magnifications of the areas boxed in L-N. (R, S) High magnification views of DiI-labeled projections arising from the hippocampal formation at different levels of the fornix pathway: fornix (F), postcommissural fornix (PF). The observed patterns correlate tightly with the sites of Sema3E-AP binding.

Other sites of Sema3E-AP binding detected are in the ventrolateral cortex (Ctx in C, D, L-N), striatum (St in C, L-N), fasciculus retroflexus (fr in D), amygdala (Am in L, N) and anterior commissure (ac in M).

(T, U) Sema3E-AP binding to brain sections is abolished in PlexinD1 null-mutant embryos, demonstrating that PlexinD1 is the predominant binding component for Sema3E in brain. The staining visualized in PlexinD1 mutant brain corresponds to that obtained using control AP fusion protein (not shown).

Scale bars: 650 μm (A-C, M-O, U, V), 100 μm (D-L, S-T).

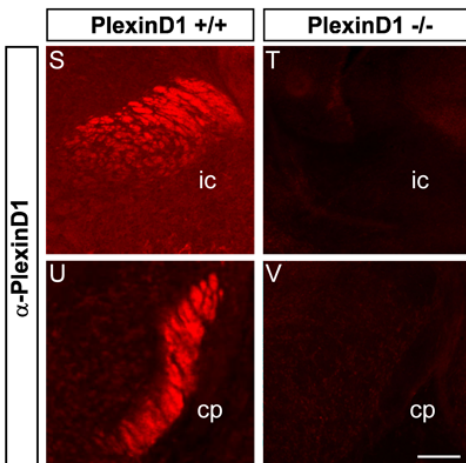
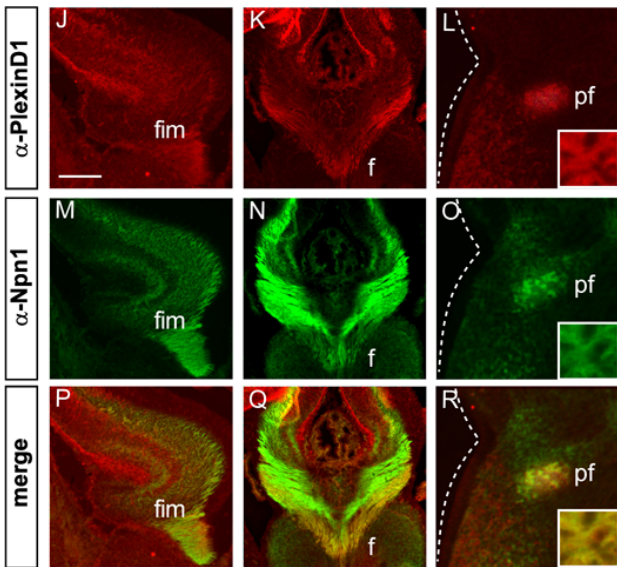
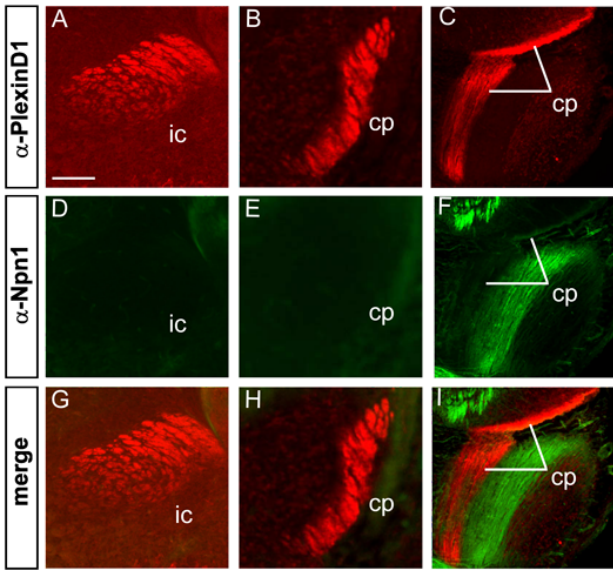


Suppl. Fig. 2: Developmental study of expression of mRNAs for candidate Sema3E receptors

Coronal sections of wild-type mouse brain were taken through the globus pallidus and thalamic reticular nucleus (A-C), through the left hemisphere (D-I), through the dorsal cortex (J-L) and through the hippocampal formation (M-U). Sections were taken at E15.5 (D, G, M, P, S), E17.5 (A-C, E, H, N, Q, T) and P2 (F, I-L, O, R, U). They were hybridized with probes for: *Sema3E* (A, M-O), *Dlx1* (B), *Er81* (C), *PlexinD1* (D-F, K, P-R) and *Npn-1* (G-I, L, S-U). (J) Cresyl violet staining to visualize the six cortical layers.

As reported, *Dlx1* labels the TRN while *Er81* labels the GP (Sussel et al., 1999; Jones and Rubenstein, 2004). *Sema3E* is expressed in both areas between which corticofugal and striatonigral axons must pass (A-C). *Sema3E* is also expressed in CA1 and CA3 pyramidal neurons adjacent to the subiculum (N). In the cortex, *PlexinD1* mRNA is first detected in the ventrolateral regions and its expression spreads medially over time (D-F). By P2, in situ hybridization signal is detected throughout the neocortex, within which *PlexinD1* expression marks layer 5 neurons, as previously reported (Chen et al., 2005). In the hippocampal formation, particularly intense staining for *PlexinD1* is observed in the pyramidal layer of the subiculum (P-R). Note that subicular neurons, but not cortical and striatal neurons, co-express *PlexinD1* and *Npn-1* (compare T with H).

Ctx: cortex, CA1 and CA3: cornus ammonis 1 and 3, DG: dentate gyrus; GP: globus pallidus, Hip: hippocampus, ic: internal capsule, St: striatum, Sub: subiculum, TRN: thalamic reticular nucleus. Scale bar: 500 μm (D-I), 250 μm (M-U), 100 μm (A-C), 50 μm (J-L).



Suppl. Fig. 3: Expression of candidate receptor proteins along descending forebrain tracts

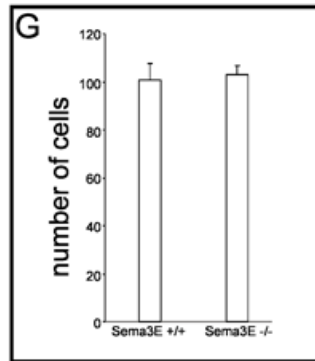
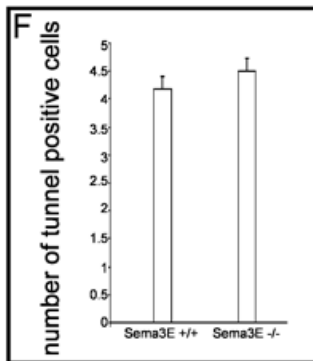
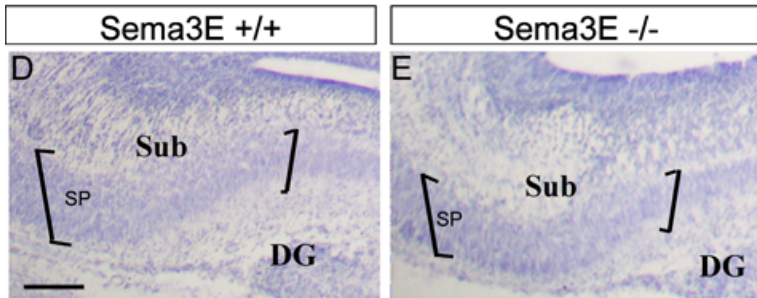
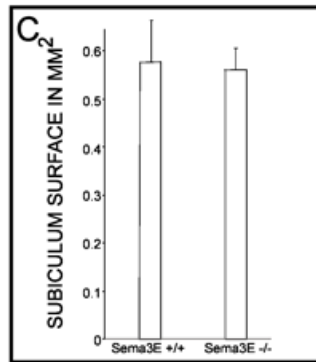
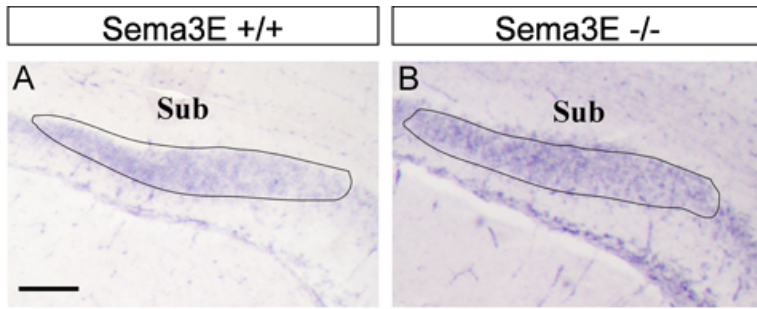
Coronal sections of wild-type brain at E17.5 were incubated with antibodies to the candidate receptor components PlexinD1 (A-C, G-I, J-L, P-R, S-V) and Npn-1 (D-I, M-R).

(A-I): High-magnification views of immunostaining with anti-PlexinD1 and anti-Npn-1 at different levels of the corticofugal and striatonigral pathways: internal capsule (A, D, G), cerebral peduncles (B, C, E, F, H, I). Merged images show that PlexinD1 is expressed throughout the corticofugal and striatonigral projections but that it is not co-expressed with Npn-1 in these fiber tracts.

(J-R): High-magnification views of immunostaining with anti-PlexinD1 and anti-Npn-1 at different levels of the subiculo-mammillary body tract: fimbria (J, M, P), fornix (K, N, Q), and postcommissural fornix (L, O, R). Merged images show that PlexinD1 is co-localized with Npn-1 along the full length of the subiculo-mammillary tract. Inset panels in L, O, R show overlap in individual axonal fascicles.

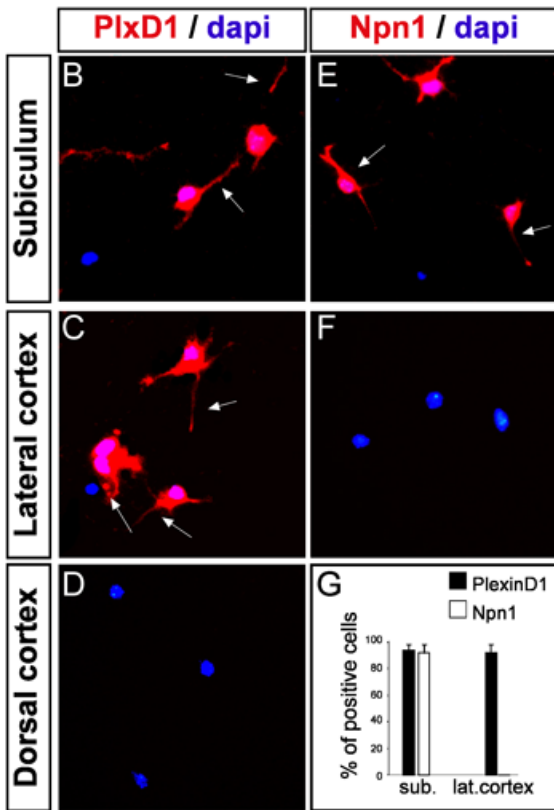
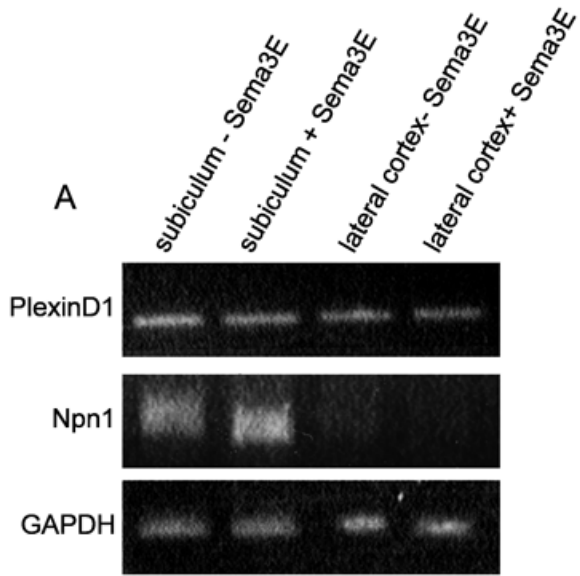
(S-V): Coronal sections of wild-type (S, U) and *PlexinD1*^{-/-} (T, V) brains at E17.5 immunostained using the anti-PlexinD1 antibody. No staining was apparent in the absence of PlexinD1.

cp: cerebral peduncles, fim: fimbria, f: fornix, ic: internal capsule, pf: postcommissural fornix. Scale bars: 100 μ m



Suppl. Fig. 4: No evidence for loss of subicular neurons in Sema3E null embryos.

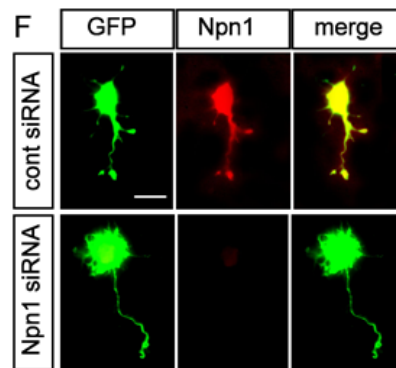
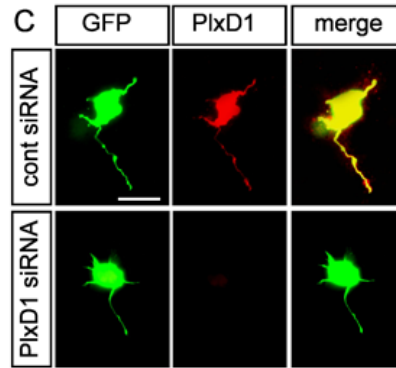
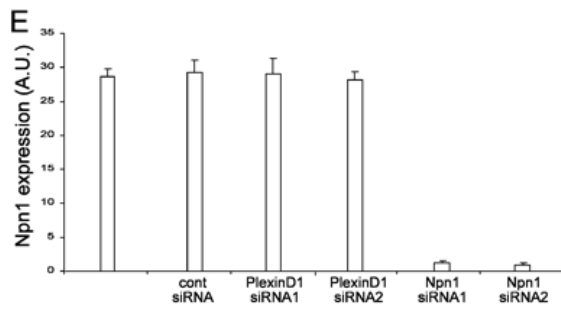
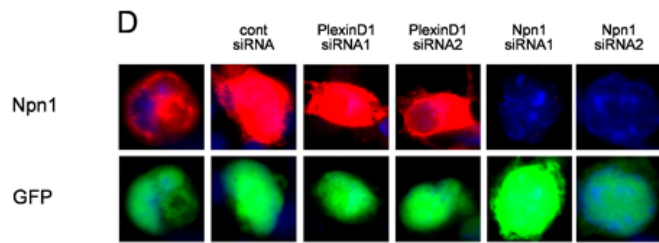
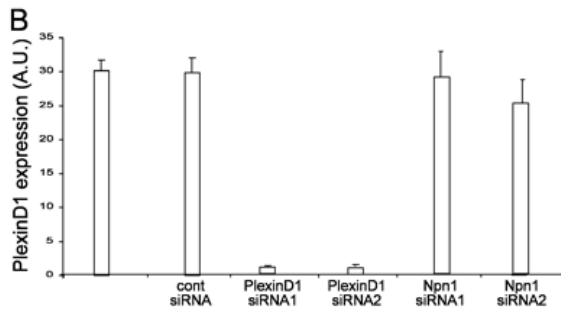
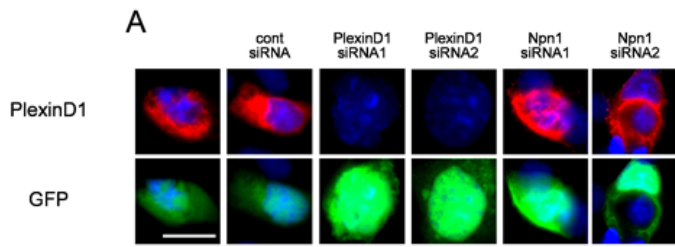
(A-B) *PlexinD1* mRNA expression in the pyramidal layer of the subiculum in E17.5 *Sema3E*^{-/-} and wild-type embryos. (C) Quantification of the surface of the pyramidal cell layer of the subiculum in ten different sections. Data are mean areas \pm s.e.m. (n=10 sections). (D-E) Cresyl violet staining shows the thickness and lamination of the subiculum to be normal in coronal sections of E17.5 *Sema3E*^{-/-} subiculum as compared to wild-type. (F, G) Quantification of the number of TUNEL-positive cells (F) or number of cells (G) in a fixed column of the subiculum in ten different sections. Data are mean number of cells \pm s.e.m. (n=10 sections). DG: dentate gyrus, sp: stratum pyramidale, Sub: Subiculum. Scale bar: 120 μ m.



Suppl. Fig. 5: Expression of PlexinD1 and Npn-1 in cultured neurons from the cortex and subiculum.

(A) RT-PCR analysis of PlexinD1 and Npn-1 expression in cultured neurons from the ventrolateral cortex and subiculum. Total RNA from neurons of the ventrolateral cortex and subiculum cultured for 2 days in the presence or absence of 5 nM Sema3E was isolated and analyzed for the expression of *PlexinD1* and *Npn-1* mRNAs. *GAPDH* mRNA was used as an internal control.

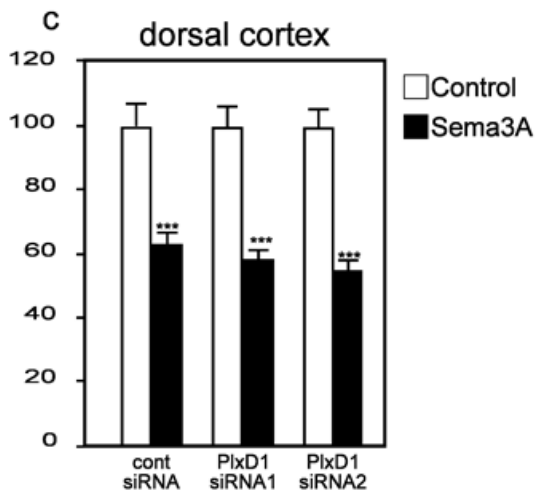
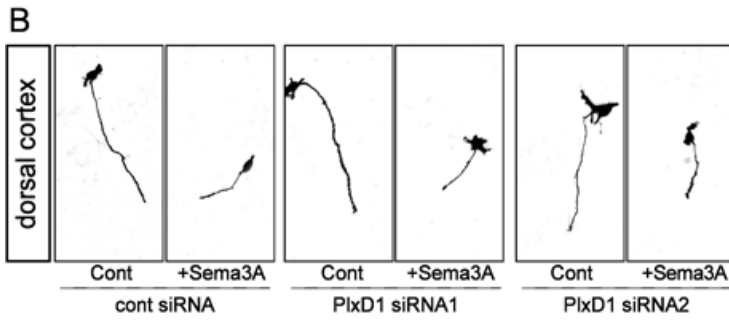
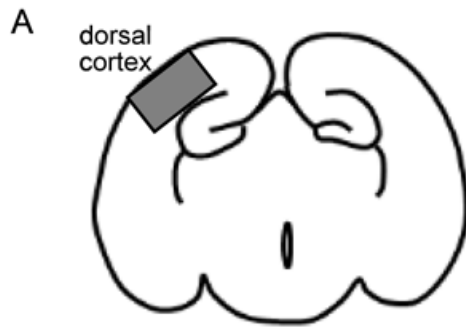
(B-G) Neurons from the subiculum, ventrolateral cortex and dorsal cortex were cultured for 24 hours and incubated with antibodies to the candidate receptor components PlexinD1 (B-D) and Npn-1 (E-F). (G) Quantification of the percentage of PlexinD1 and Npn1-immunopositive neurons (means \pm SEM). Subicular neurons express both PlexinD1 and Npn-1, whereas cortical neurons express only PlexinD1.



Suppl. Fig. 6: Controls for specificity of knockdown of PlexinD1 and Npn-1 by small interfering RNAs.

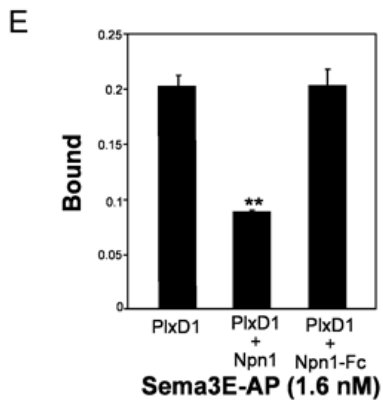
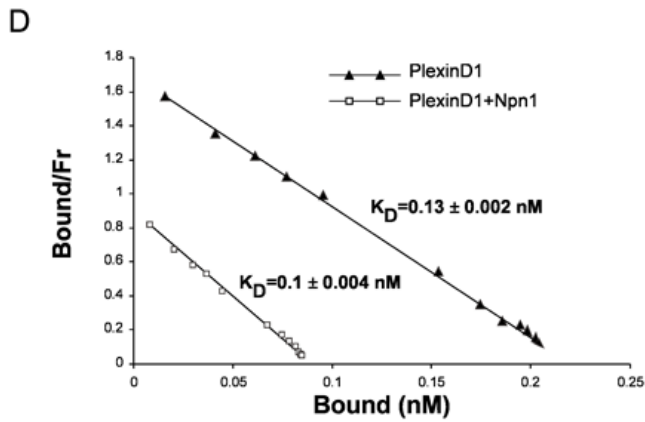
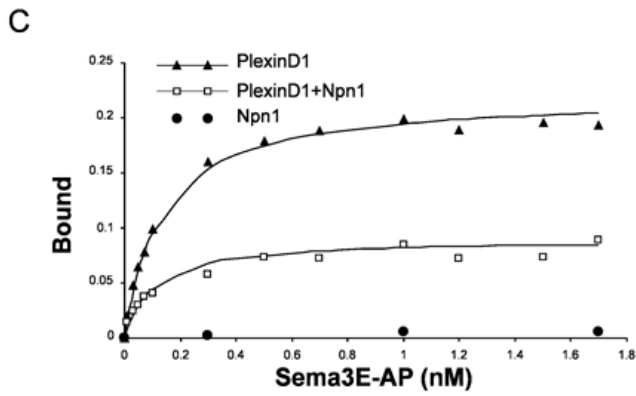
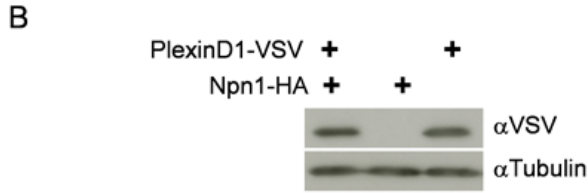
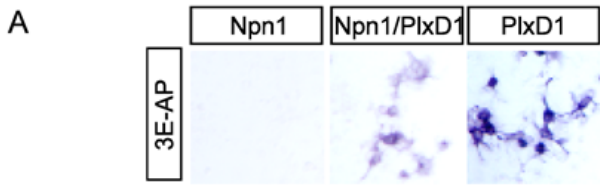
(A) Typical images of COS-7 cells co-transfected with expression vectors for GFP and PlexinD1, together with the indicated siRNAs. GFP expression (green) was not affected by any siRNA, whereas PlexinD1 expression (red) was massively reduced by both PlexinD1 siRNAs. Control and Npn-1 siRNAs were without effect. Nuclei are visualized using DAPI (blue). (B) Quantitative analysis of PlexinD1 levels in the experiments illustrated in A (means \pm s.e.m.). (C) Dissociated subicular neurons were electroporated with a GFP expression vector to identify transfected neurons together with control or PlexinD1 siRNAs. Targeted, but not control, siRNAs led to disappearance of immunoreactivity for PlexinD1 without affecting GFP immunoreactivity. (D) Typical images of COS7 cells co-transfected with expression vectors for GFP (green) and Npn-1-HA (red), together with the indicated siRNAs. Npn-1 expression was massively reduced by both Npn-1 siRNAs, whereas control and PlexinD1 siRNAs were without effect. (E) Quantitative analysis of Npn-1-HA levels in the experiments illustrated in D (means \pm SEM). (F) Dissociated subicular neurons were co-electroporated with GFP expression vector and control or Npn-1 siRNAs. Npn-1 siRNAs gave complete, specific knockdown of endogenous Npn-1.

Methods: COS-7 cells co-transfected with the indicated siRNA duplexes using Lipofectamine Plus (Invitrogen). 48 hr after transfection, cells were fixed and immunostained with rabbit anti-PlexinD1 antibodies (1:100) or rat anti-HA antibodies (1:300). Secondary antibodies were goat Cy3-conjugated anti-rabbit and anti-rat (1:500 Jackson Immuno Research). Pictures were taken with a LEICA DM IRB camera and fluorescence intensity was determined using the ImageJ software. Means values are plotted (means \pm s.e.m.). Scale bar: 30 μ m



Suppl. Fig. 7: Effects of PlexinD1 siRNAs on responses to Sema3A

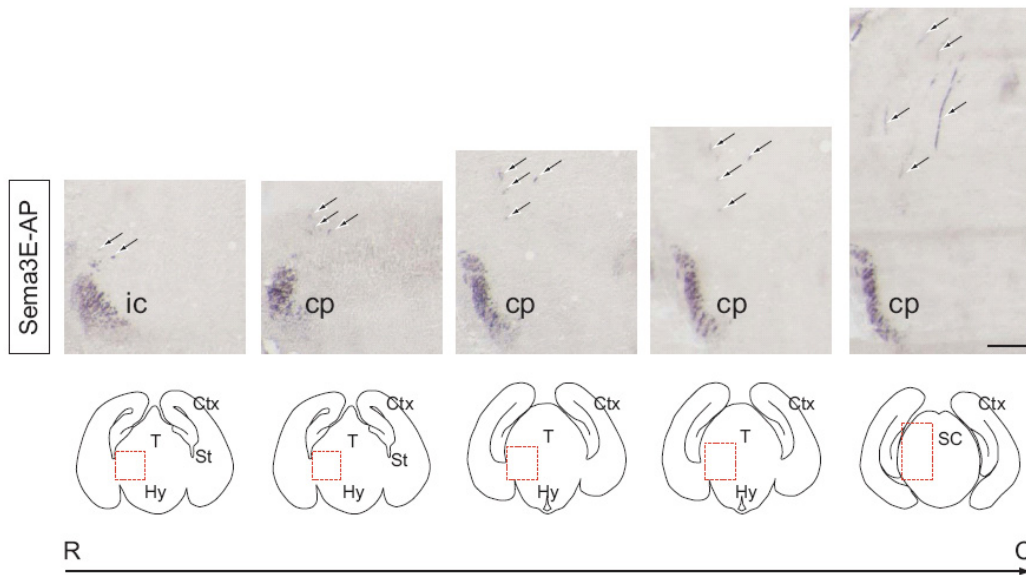
(A) Schematic diagram of coronal section through E17.5 brain illustrating the dorsal region of the cortex dissected for *in vitro* assay. (B) Typical images of dissociated dorsal cortical neurons cultured in the presence or absence of 5 nM Sema3A after co-electroporation of GFP expressing vector and the indicated siRNA. (C) Quantitative analysis of axon length of cortical neurons after electroporation of the indicated siRNA. Knock-down of PlexinD1 does not affect the inhibitory effect of Sema3A on axon growth. Mean axonal lengths \pm SEM are presented, normalized to 100% for values obtained in control conditions.



Suppl. Fig. 8: Binding affinity of Sema3E for PlexinD1 and Npn-1.

(A) Binding of Sema3E-AP to COS-7 cells expressing Npn-1 or PlexinD1 alone or both. No binding is seen to Npn-1 alone whereas the strong binding to PlexinD1 is reduced in the presence of Npn-1. (B) VSV-PlexinD1 is expressed at similar levels at the surface of COS-7 cells when transfected with an empty vector or with a vector encoding HA-Npn-1, as visualised by Western blotting using an anti-VSV antibody. (C) Sema3E-AP binding curves reveal that co-expression of Npn-1 and PlexinD1 in COS-7 cells results in a decrease in the number of binding sites (B_{max}) by a factor of ~ 2 , compared to cells expressing PlexinD1 alone. The amount of bound AP-activity was determined colorimetrically. (D) The binding data were plotted by the method of Scatchard. The apparent K_D values for the interactions between Sema3E-AP and PlexinD1, or PlexinD1 together with Npn-1, were 0.13 ± 0.002 nM (mean \pm s.e.m.; $n=3$) and 0.10 ± 0.004 nM (mean \pm s.e.m.; $n=3$), respectively. (E) Quantification of Sema3E-AP binding to COS-7 cells co-expressing PlexinD1 and Npn-1, and expressing PlexinD1 alone in the presence or absence of 2 μ g/ml Npn1-Fc (means \pm SEM). Unlike full length Npn-1, soluble Npn-1-Fc does not induce significant change in the number of binding sites for Sema3E-AP. **significantly different with $p < 0.01$.

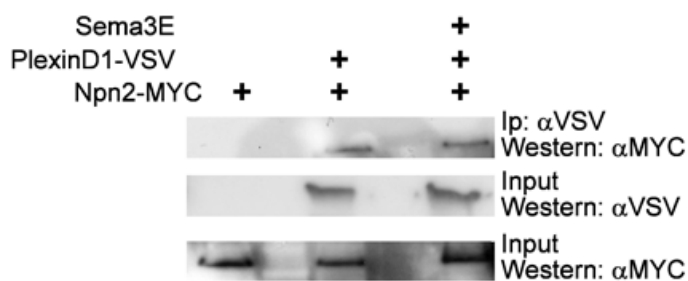
Methods: COS-7 cells were transfected with VSV-PlexinD1 and/or HA-Npn-1 expression vectors using Lipofectamine Plus (Invitrogen). To quantify surface expression of PlexinD1, cell surface proteins were labeled by biotinylation (Pierce Biotechnology). Cell lysates were immunoprecipitated with neutravidin beads (Pierce Biotechnology) and Western-blotted with mouse anti-VSV antibody (gift from A. Lebivic). Saturation equilibrium binding studies were performed as described (Flanagan and Leder, 1990).



Suppl. Fig. 9: Ectopic axon fascicles in *Sema3E* null embryos.

Serial sections of a *Sema3E*^{-/-} E17.5 embryo in which the *Sema3E*-AP-labeled fascicles can be traced from the internal capsule (arrows in left panel) to their ectopic endpoint in the dorsal midbrain (arrows in right panel).

cp: cerebral peduncle, Ctx: cortex, Hy: hypothalamus, ic: internal capsule, R->C: rostro-caudal axis, SC: superior colliculi, St: striatum, T: thalamus.



Suppl. Fig. 10: Npn-2 and PlexinD1 interact

Co-immunoprecipitation experiments showing that PlexinD1 can form a complex with Npn-2 in both the presence and absence of Sema3E. COS-7 cells were transfected with the indicated combinations of Myc-tagged Npn-2 and VSV-tagged PlexinD1, and treated or not with Sema3E (5 nM).

Supplemental References

Flanagan, J. G., and Leder, P. (1990). The kit ligand: a cell surface molecule altered in steel mutant fibroblasts. *Cell* 63, 185-194.

Jones, E. G., and Rubenstein, J. L. (2004). Expression of regulatory genes during differentiation of thalamic nuclei in mouse and monkey. *J Comp Neurol* 477, 55-80.

Sussel, L., Marin, O., Kimura, S., and Rubenstein, J. L. (1999). Loss of Nkx2.1 homeobox gene function results in a ventral to dorsal molecular respecification within the basal telencephalon: evidence for a transformation of the pallidum into the striatum. *Development* 126, 3359-3370.